Apatite fission track data from northern Hogem batholith, Quesnel terrane, north-central British Columbia: A progress report

Xi Wang[1], Ruohong Jiao[1], and Luke Ootes[2]

[1] School of Earth and Ocean Sciences, University of Victoria, Victoria, BC, V8W 3P6
[2] British Columbia Geological Survey, Ministry of Mining and Critical Minerals, Victoria, BC, V8W 9N3
[a] corresponding author: xiw@uvic.ca

Recommended citation: Wang, X., Jiao, R., and Ootes, L., 2025. Apatite fission track data from northern Hogem batholith, Quesnel terrane, north-central British Columbia: A progress report. In: Geological Fieldwork 2024, Ministry of Mining and Critical Minerals, British Columbia Geological Survey Paper 2025-01, pp. 85-91.

Abstract

The intrusive history of the northern Hogem batholith has been well-documented through previous bedrock mapping and U-Pb zircon and $^{40}Ar/^{39}Ar$ geochronology. However, the post-emplacement cooling history and exhumation of the batholith remain unknown. This study presents preliminary results of apatite fission track analyses from four mapped intrusive suites: Thane Creek (207-194 Ma); Duckling Creek (182-175 Ma); Osilinka (<160 Ma); and Mesilinka (135-128 Ma). Analysis of separated apatite yielded fission track ages of 46 and 26 Ma (Thane Creek suite, two samples); 69 and 100 Ma (Duckling Creek suite, two samples); and 60, 49, and 43 Ma (Mesilinka suite, three samples); Osilinka suite samples failed to yield apatite. Combining these ages with track length distribution data from five samples, as well as the U-Pb zircon crystallization ages and $^{40}Ar/^{39}Ar$ ages, we modelled the cooling history of the samples. Our results indicate that following initial magma cooling in the Jurassic and Cretaceous, northern Hogem batholith experienced continuous cooling from ca. 60-40 Ma until the present as it exhumed to shallow crustal levels.

Keywords: Hogem batholith, Quesnel terrane, low-temperature thermochronology, apatite fission track, LA-ICP-MS

1. Introduction

Hogem batholith, north-central Quesnel terrane, hosts porphyry Cu (±Au, Mo) mineralization and has received recent bedrock mapping and supporting geochronological studies (e.g., Bath et al., 2014; Devine et al., 2014; Jones, 2022; Jones et al., 2022, 2023; Ootes et al., 2020a-c). Although new $^{40}Ar/^{39}Ar$ cooling ages have been presented (Ootes et al., 2020a, 2020b; Jones, 2022; Jones et al., 2022) the post-emplacement low-temperature cooling history of the batholith remains uncertain. Because porphyry deposits typically develop at shallow crustal depths, understanding the exhumation history of Hogem batholith can help guide future exploration and provide insights into the low-temperature tectonic evolution of this part of the Cordilleran orogen. This project aims to estimate the thermal history of the batholith, which will help resolve spatial and temporal patterns of exhumation processes. Herein we report preliminary apatite fission track data from samples collected during previous bedrock mapping (Ootes et al., 2020a-c) and use these data to model time-temperature paths.

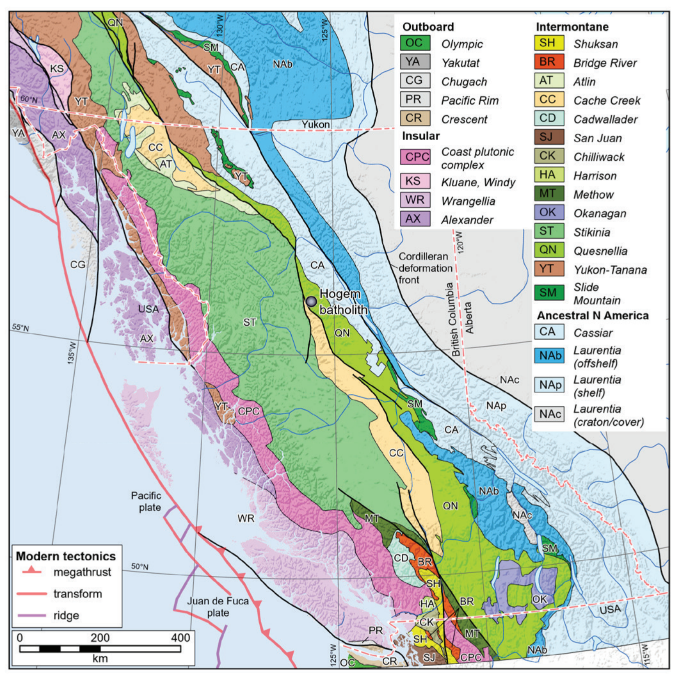

Fig. 1. Location of Hogem batholith. Terranes modified from Colpron (2020).

2. Geological setting

Northern Hogem batholith is near the western flank of Quesnel terrane in north-central British Columbia (Fig. 1) in an area that includes overlapping territories of many Indigenous Nations. Quesnel terrane consists of an assemblage of Paleozoic basement rocks that are unconformably overlain by Upper Triassic to Lower Jurassic volcanic, sedimentary, and intrusive rocks (e.g., Schiarizza et al., 2001). The terrane is considered to have formed in the Paleozoic as an island arc system and later amalgamated with other terranes (Stikine, Cache Creek, and Yukon-Tanana) to form the larger Intermontane Superterrane during the Late Triassic to Early Jurassic (Mihalynuk et al., 1994). The accretion of the Intermontane Superterrane to North America is thought to have occurred either during the Early to Middle Jurassic (Evenchick et al., 2007; Monger and Gibson, 2019) or the Late Cretaceous (Johnston, 2008; Hildebrand, 2009; Chen et al., 2019).

Hogem batholith is bordered to the north and east by volcanic and sedimentary rocks of the Nicola Group (Triassic), with both faulted and intrusive contacts (Fig. 2; Ootes et al., 2020a, c). On the western side, the batholith and the Nicola Group are juxtaposed against the Cache Creek and Stikine terranes along the Pinchi-Ingenika dextral strike-slip fault system.

Building on previous mapping and geochronologic studies (Devine et al., 2014; Ootes et al., 2020a, b; Jones et al., 2021b, 2023) our study focuses on the four intrusive suites that have been identified in northern Hogem batholith. These include dioritic rocks assigned to Thane Creek (207 to 194 Ma), biotite-pyroxenite and syenite of the Duckling Creek (182 to 174 Ma), leucocratic equigranular granite of the Osilinka (<160 Ma), and tonalite, granodiorite, and granite of the Mesilinka (135 to 127 Ma; Fig. 2). Detailed descriptions of each suite can be found in Ootes et al. (2020a, c).

3. Methods and samples

Low-temperature thermochronology includes a suite of radiometric dating techniques that are used to study the thermal evolution of rocks and minerals at relatively low temperatures (typically between ~30 and 350°C). Fission-track dating is one of these methods. When a ^{238}U nucleus undergoes fission, it splits into two smaller fragments, which leave behind visible tracks as they pass through the mineral structure (Fleisher et al., 1975). Fission-track dating is based on analyzing microscopic damage trails (fission tracks) that are created by the spontaneous fission of ^{238}U atoms within the crystal. The annealing and preservation of fission tracks in crystals are controlled by temperature and time. Therefore, measured track density and length distribution data can be used to estimate the time-temperature paths of the host rocks. In apatite, fission tracks are partially annealed and preserved in the temperature range of 60-110°C (Laslett, 1987), making it an ideal tool for constraining cooling processes in the upper crust (3-5 km).

3.1. Samples

The samples collected during previous bedrock mapping that we analyzed consist of felsic to intermediate rocks, such as granite, diorite, and syenite (Table 1). The mineral separates were processed through standard magnetic and density separation to obtain pure apatite grains. Although we attempted to produce fission track data from all four suites, samples from the Osilinka suite failed to yield apatite.

3.2. Apatite fission track analysis

The apatite fission track analysis was performed at the University of Victoria. Apatite grains were mounted in epoxy on glass slides. Following grinding and polishing to reveal internal surfaces, spontaneous tracks were etched using 5.5 M HNO_3 at 21°C for 20 seconds (see Donelick et al., 2005). Fission track density and length were measured on polished sample surfaces (Figs. 3a, b) using Autoscan Automated Counting Systems, which are based on Zeiss Axio Imager microscope at a magnification of 1000x with a dry objective. Surface tracks are used to determine track density. D_{par}, a parameter that assesses

Table 1. Thane Creek, Duckling Creek, and Mesilinka suite samples analyzed in this study; U-Pb zircon and ^{40}Ar/^{39}Ar ages are for intrusive suites, not individual samples. U-Pb zircon ages from Jones et al. (2022) and ^{40}Ar/^{39}Ar ages from Ootes et al. (2020b); apatite fission track ages from this study.

ID	Sample	Latitude (°N)	Longitude (°W)	Elevation (m)	Intrusive suite	Rock Type	U-Pb age (ca. Ma)	^{40}Ar/^{39}Ar age (ca. Ma)	Apatite FT (Ma)
Ms-1	18ab8-4	56.223	-125.984	1945	Mesilinka	Biotite phenocrystic tonalite	135	110	60 ±13
Ms-2	18lo12-7	56.224	-125.923	1643	Mesilinka	Porphyritic granite	130	110	43 ±8
Ms-3	19AB17-3	56.355	-126.162	1754	Mesilinka	K-feldspar phenocrystic granite	130	110	49 ±7
DCs-1	19GJ13-4	56.004	-125.571	1857	Duckling Creek	Syenites	180	177	69 ±23
DCs-2	19GJ13-5a	55.999	-125.526	1722	Duckling Creek	Syenite	180	177	100 ±18
TCs-1	19GJ12-4	56.212	-125.646	1912	Thane Creek	Quartz diorite	200	125	26 ±4
TCs-2	19GJ13-3	56.024	-125.599	1797	Thane Creek	Quartz monzodiorite	200	125	46 ±13

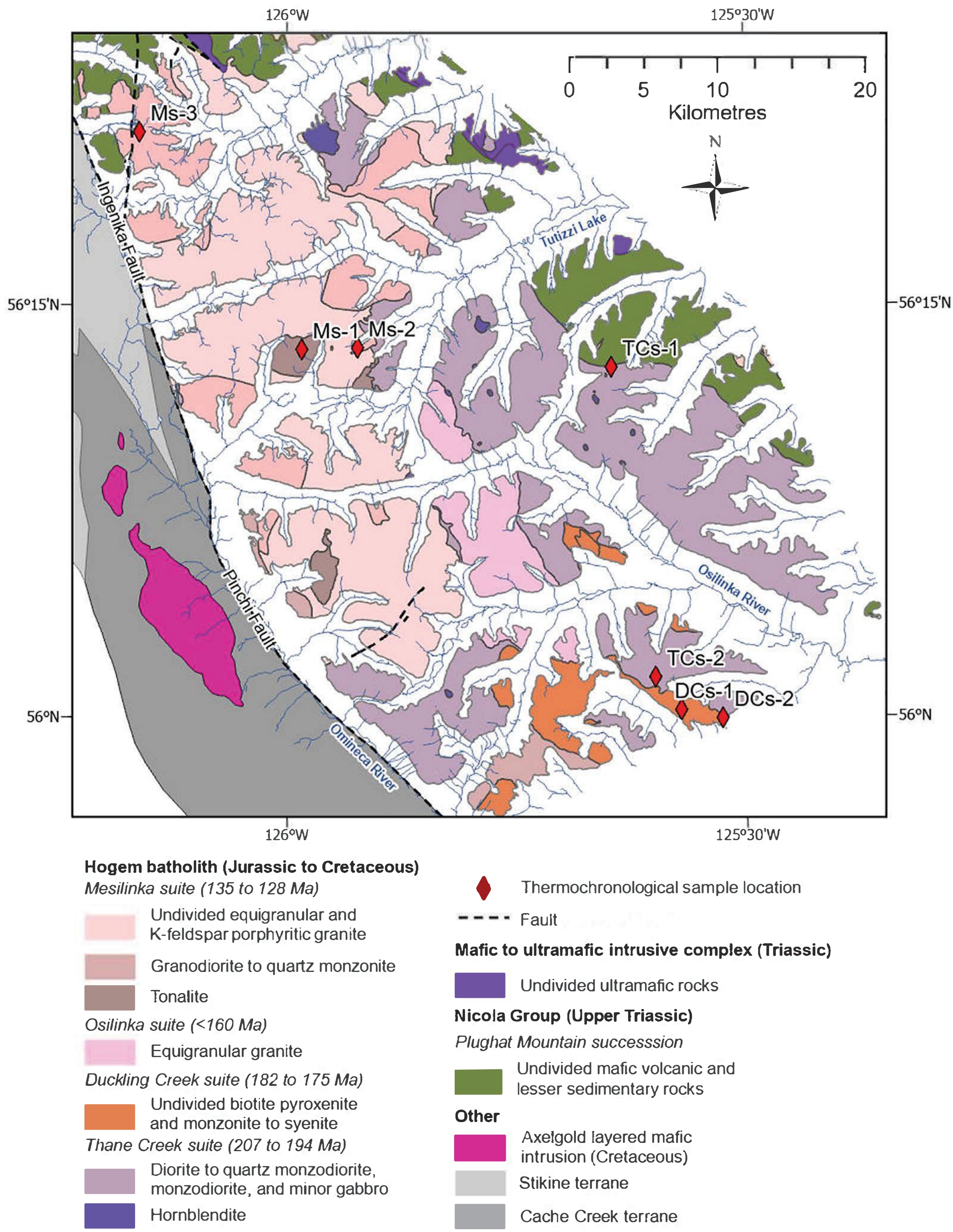

Fig. 2. Geology of northern Hogem batholith area and sample locations. Modified after Ootes et al. (2020c).

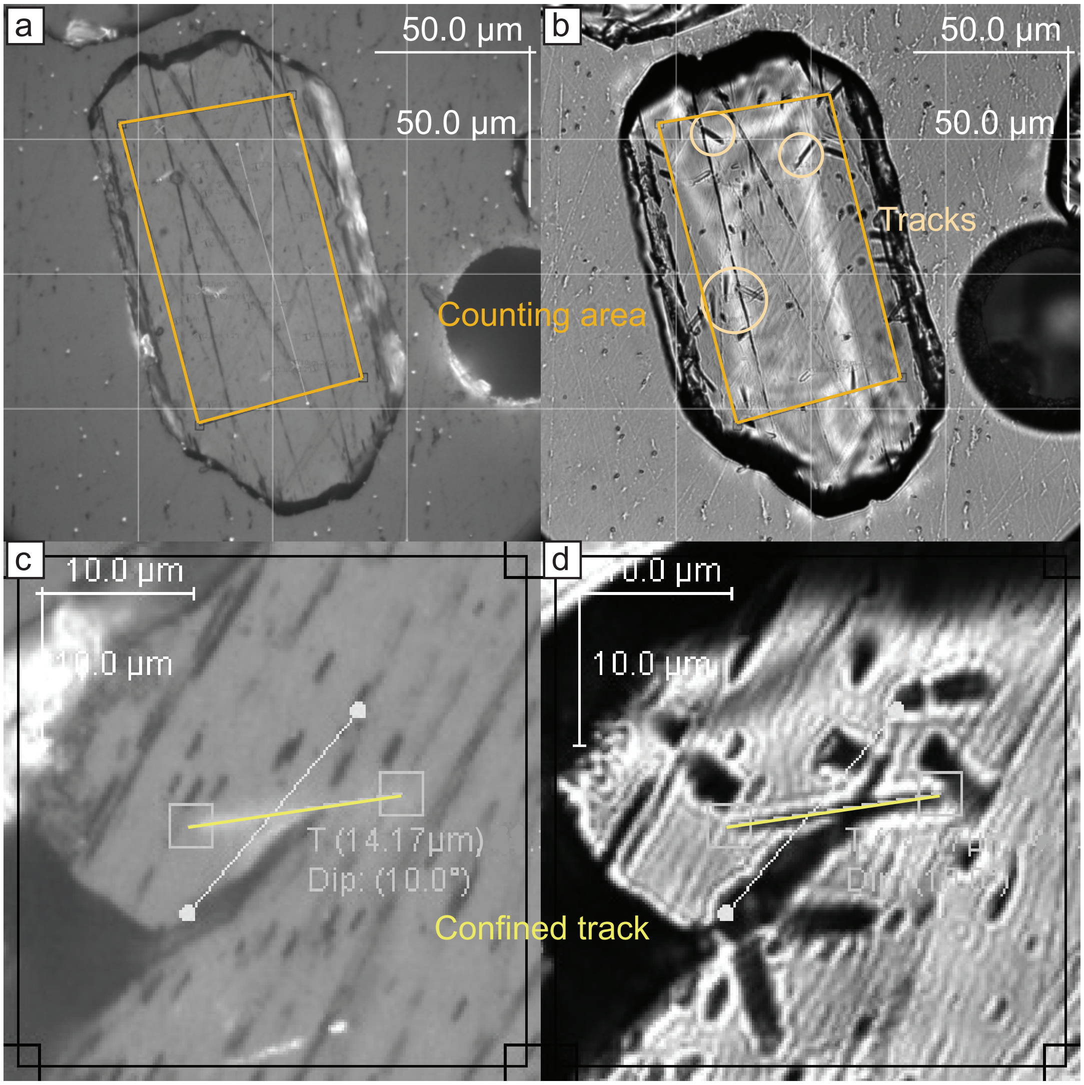

Fig. 3. Images from a Zeiss Axio Imager microscope under transmitted light (**a** and **c**) and cross-polarized light (**b** and **d**). **a)** and **b)** Apatite from this study, showing the area, outlined in orange, used for measuring fission track density, track length, and uranium (U) content; **c)** and **d)** An example of a confined fission track, traced in yellow, with its length measured for thermal history modelling.

the impact of annealing, was measured as the maximum diameter of the etch pits parallel to the crystallographic c-axis. Where possible, confined tracks (fission tracks fully retained within a crystal grain without intersecting the surface) were measured to evaluate the track length distribution (Figs. 3c, d). Track density and track length distribution from each sample are used to provide thermal information for modelling. The concentration of ^{238}U was determined by LA-ICP-MS, calibrated using National Bureau of Standards trace element glasses NIST 611, 613, and 615 as standards, following the method described by Hasebe et al. (2004).

3.3. Thermal history modelling

We modelled the cooling history of the samples using the acquired apatite fission track age and length data. The modelling process employs a Bayesian transdimensional Markov Chain Monte Carlo method to estimate the time-temperature (t-T) paths that best explain the observed data (see Gallagher, 2012). This method generates a series of possible thermal histories (t-T paths) and evaluates the likelihood of each thermal history by comparing the predicted and observed fission track data. Each thermal history is represented by a path created from a set of t-T points that describe the rock's cooling and heating through time. We used the apatite fission track annealing model of Ketcham et al. (2007), with D_{par} as a kinetic parameter, which defines how fission tracks in apatite shorten with time and temperature. The modelled results represent the range of plausible thermal histories. The modelling method also assesses the model complexity and avoids overfitting by penalizing models with more time-temperature points. In our analyses, inversion of each sample included 200,000 Monte Carlo iterations, with the first 100,000 iterations discarded as the 'burn-in' phase, and the remaining iterations used for the 'post-burn-in' analysis.

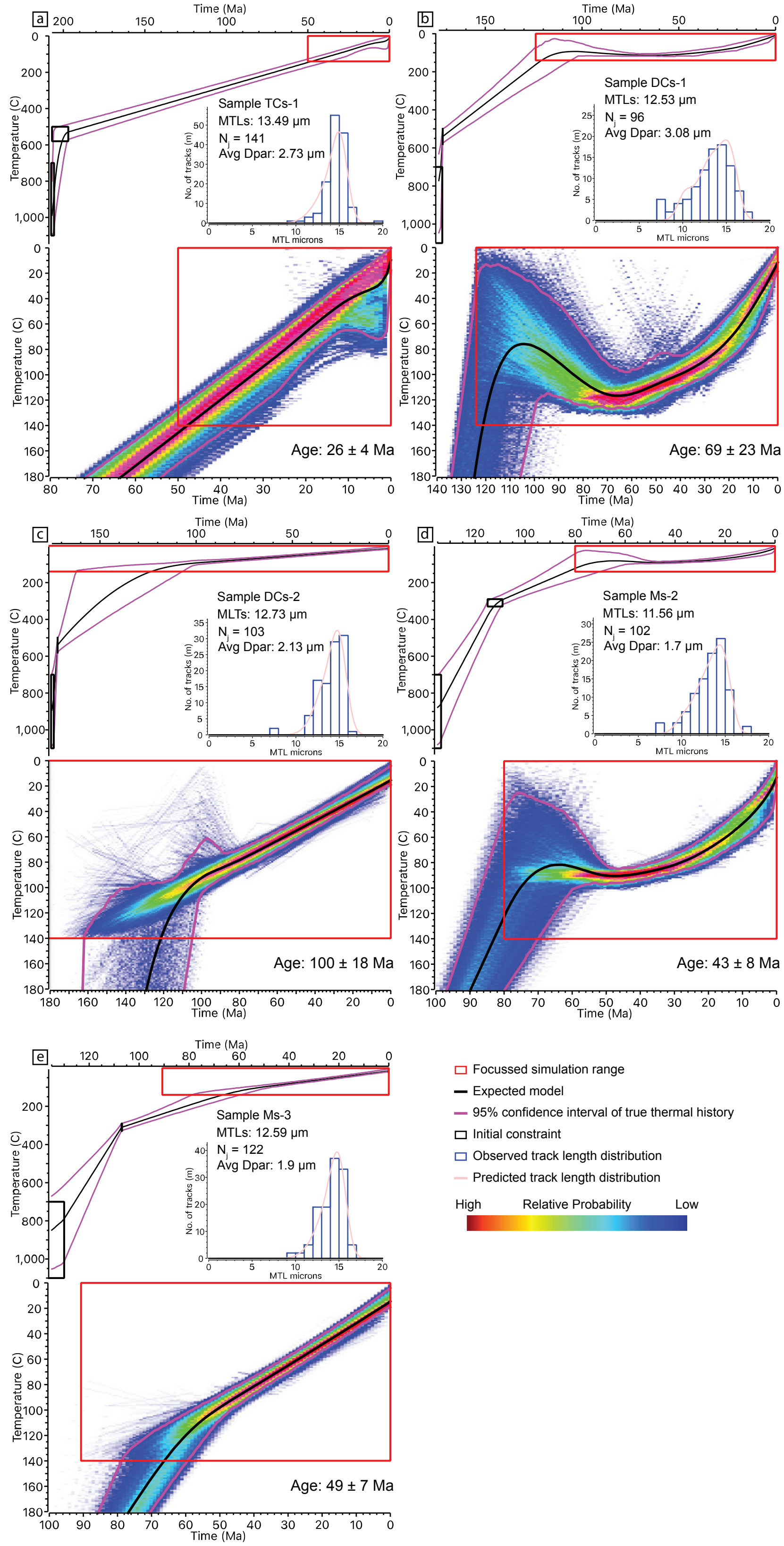

Fig. 4. Thermal history modelling of apatite fission track data for five samples using Quantitative Thermochronology Qt (QTQt) software. **a)** Thane Creek suite; **b)** and **c)** Duckling Creek suite; **d)** and **e)** Mesilinka suite. Large red boxes in the lower part of each diagram are close-ups of the small red boxes in the upper parts and represent the focused ranges in time-temperature space for apatite fission track simulations. MTLs = mean track lengths length; N_j = number of confined tracks counted; D_{par} = maximum diameter of the etch pits parallel to the crystallographic c-axis.

The boundary conditions for our thermal modelling include a present-day mean surface temperature of 10 ±10°C, ages from previous studies (Table 1), and closure temperatures of 900 ±200°C for U-Pb zircon (Cherniak and Watson, 2001), 540 ±40°C for ^{40}Ar/^{39}Ar hornblende (Harrison, 1982), and 310 ±20°C for ^{40}Ar/^{39}Ar biotite (Harrison et al., 1985).

4. Results

Seven bedrock samples yielded sufficient apatite grains for fission track analysis, and the determined ages ranged between 100 and 26 Ma (Table 1). We present new results, together with the U-Pb zircon crystallization ages, ^{40}Ar/^{39}Ar hornblende cooling ages, and a possible post-deformation ^{40}Ar/^{39}Ar biotite from previous studies (Table 1) in Figure 4. Five out of the seven samples with sufficient confined fission track lengths (>95) were selected for thermal modelling (Fig. 4).

4.1. Thane suite

Samples from the Thane Creek suite yielded apatite fission track ages of 26 ±4 Ma (sample TCs-1) and 46 ±13 Ma (sample TCs-2). The mean track length for sample TCs-1 is 13.36 ±1.60 µm. The thermal history modelling result of TCs-1 shows cooling since modelled age constraint (50 Ma) without residence in the apatite fission track partial annealing zone (Fig. 4a).

4.2. Duckling Creek suite

Samples from the Duckling Creek suite yielded apatite fission track ages of 69 ±23 Ma (sample DCs-1) and 100 ±18 Ma (sample DCs-2). The mean track lengths are 12.36 ±3.27 µm (sample DCs-1) and 12.44 ±2.32 µm (sample DCs-2). Thermal history modelling results (Figs. 4b, c) show cooling starting at 100-70 Ma, with a possible pronounced residence in the apatite fission track partial annealing zone before ca. 80 Ma.

4.3. Mesilinka suite

Samples from the Mesilinka yielded apatite fission track ages of 60 ±13 Ma (sample Ms-1); 43 ±8 Ma (sample Ms-2) and 49 ±7 Ma (sample Ms-3). The mean track lengths for sample Ms-2 is 11.37 ±3.75 µm, and for sample Ms-3 is 12.45 ±2.21 µm. The thermal history modelling results of Ms-2 and Ms-3 (Figs. 4d, e) show cooling starting at ca. 50 Ma with a possible earlier prolonged residence in the apatite fission track partial annealing zone.

5. Summary

Zircon U-Pb crystallization ages, along with hornblende and biotite ^{40}Ar/^{39}Ar ages, indicate initial magma cooling between approximately 200 and 110 Ma (Late Triassic to Early Cretaceous; Table 1). Most of our apatite fission track ages and thermal history models indicate that northern Hogem batholith experienced continuous cooling since 60-40 Ma, with some samples suggesting a prolonged time in the partial annealing zone before cooling (ca. 80-50 Ma; Fig. 4). Future work will collect apatite and zircon (U-Th)/He ages from the batholith, along with more apatite fission track and apatite and zircon (U-Th)/He data from north of Hogem batholith and from central Quesnel terrane.

Acknowledgments

This project is funded by EMLI-UVic Partnership Fund. This is a contribution to the Hogem mapping project of the British Columbia Geological Survey. The authors thank Lawrence B. Aspler and Eva Enkelmann for constructive reviews and comments that helped improve the paper.

References cited

Bath, A.B., Cooke, D.R., Friedman, R.M., Faure, K., Kamenetsky, V.S., Tosdal, R.M., and Berry, R.F., 2021. Mineralization, U-Pb geochronology, and stable isotope geochemistry of the Lower Main zone of the Lorraine deposit, north-central British Columbia: A replacement-style alkalic Cu-Au porphyry. Economic Geology, 109, 979-1004. <https://doi.org/10.2113/econgeo.109.5.979>

Chen, Y., Gu, Y.J., Currie, C.A., Johnston, S.T., Hung, S.-H., Schaeffer, A.J., and Audet, P., 2019. Seismic evidence for a mantle suture and implications for the origin of the Canadian Cordillera. Nature Communications, 10, article 2249. <https://doi.org/10.1038/s41467-019-09804-8>

Cherniak, D.J., and Watson, E.B., 2001. Pb diffusion in zircon. Chemical Geology, 172, pp. 5-24.

Colpron, M., 2020. Yukon terranes-A digital atlas of terranes for the northern Cordillera. Yukon Geological Survey. Available at: <https://data.geology.gov.yk.ca/Compilation/2#InfoTab>

Devine, F.A., Chamberlain, C.M., Davies, A.G., Friedman, R., and Baxter, P., 2014. Geology and district-scale setting of tilted alkalic porphyry Cu-Au mineralization at the Lorraine deposit, British Columbia. Economic Geology, 109, 939-977.

Donelick, R.A., O'Sullivan, P.B., and Ketcham, R.A., 2005. Apatite Fission-Track Analysis. Reviews in Mineralogy and Geochemistry, 58, pp. 49-94. <https://doi.org/10.2138/rmg.2005.58.3>

Evenchick, C.A., McMechan, M.E., McNicoll, V.J., and Carr, S.D., 2007. A synthesis of the Jurassic-Cretaceous tectonic evolution of the central and southeastern Canadian Cordillera: Exploring links across the orogen. In: Sears, J.W., Harms, T.A., and Evenchick, C.A., (Eds.), Whence the mountains? Inquiries into the evolution of orogenic systems: A volume in honor of Raymond A. Price. Geological Society of America Special Paper 433, pp. 117-145. <https://doi.org/10.1130/2007.2433(06)>

Fleisher, R., Price, P., and Walker, R., 1975. Nuclear tracks in solids: Principles and applications. 1st ed. University of California Press. <https://doi.org/10.2307/jj.13167934>

Gallagher, K., 2012. Transdimensional inverse thermal history modeling for quantitative thermochronology. Journal of Geophysical Research: Solid Earth, 117, B02408. <https://doi.org/10.1029/2011JB008825>

Harrison, T.M., 1982. Diffusion of ^{40}Ar in hornblende. Contributions to Mineralogy and Petrology, 78, pp. 324-331.

Harrison, T.M., Duncan, I., and McDougall, I., 1985. Diffusion of ^{40}Ar in biotite: Temperature, pressure and compositional effects. Geochimica et Cosmochimica Acta, 49, 2461-2468. <https://doi.org/10.1016/0016-7037(85)90246-7>

Hasebe, N., Barbarand, J., Jarvis, K., Carter, A., and Hurford, A.J., 2004. Apatite fission-track chronometry using laser ablation ICP-MS. Chemical Geology, 207, 135-145. <https://doi.org/10.1016/j.chemgeo.2004.01.007>

Hildebrand, R.S., 2009. Did westward subduction cause Cretaceous-Tertiary orogeny in the North American Cordillera? Geological

Society of America Special Paper, 457, 71 p. <https://doi.org/10.1130/2009.2457>

Johnston, S.T., 2008. The Cordilleran ribbon continent of North America. Annual Review of Earth and Planetary Sciences, 36, pp. 495-530. <https://doi.org/10.1146/annurev.earth.36.031207.124331>

Jones, G., 2022. Implications of in situ zircon U-Pb, Lu-Hf, oxygen-isotope, and trace element geochemistry on the petrogenetic history of the northern Hogem batholith in the Quesnel terrane, north-central British Columbia, Canadian Cordillera. Unpublished M.Sc. thesis University of Alberta, 373 p.

Jones, G.O., Pearson, D.G., Vezinet, A., Luo, Y., Stern, R.A., Milidragovic, D., and Ootes, L., 2021a. Preliminary zircon geochemistry of northern Hogem batholith, Quesnel terrane, north-central British Columbia (parts of NTS 093M/16, 093N/13, 14, 094C/03-06, 094D/01, 08). In: Geoscience BC Summary of Activities 2020: Minerals and Mining, Geoscience BC, Report 2021-01, pp. 105-120.

Jones, G., Ootes, L., Milidragovic, D., Friedman, R., Camacho, A., Luo, Y., Vezinet, A., Pearson, D.G., and Schiarizza, P., 2021b. Geochronology of northern Hogem batholith, Quesnel terrane, north-central British Columbia. In: Geological Fieldwork 2020, British Columbia Ministry of Energy, Mines and Low Carbon Innovation, British Columbia Geological Survey Paper 2021-01, pp. 37-56.

Jones, G., Ootes, L., Luo, Y., Stern, R., Vezinet, A., and Pearson, D.G., 2022. In situ zircon U-Pb, Lu-Hf, δ18O, and trace elements from intrusive units in northern Hogem batholith, Quesnel terrane, north-central British Columbia. British Columbia Ministry of Energy, Mines and Low Carbon Innovation, British Columbia Geological Survey GeoFile 2022-09, 19 p.

Jones, G., Ootes, L., Luo, Y., Vezinet, A., Stern, R., Milidragovic, D., and Pearson, D.G., 2023. The relative roles of ancient and juvenile crust in building accretionary orogens-Minimal ancient crust involved in the magmatic evolution of a North American Cordillera accreted terrane indicated by igneous zircon Hf-O. Lithos, 107213. <https://doi.org/10.1016/j.lithos.2023.107213>

Ketcham, R.A., Carter, A., Donelick, R.A., Barbarand, J., and Hurford, A.J., 2007. Improved modeling of fission-track annealing in apatite. American Mineralogist, 92, pp. 799-810. <https://doi.org/10.2138/am.2007.2281>

Laslett, G.M., Green, P.F., Duddy, I.R., and Gleadow, A.J.W., 1987. Thermal annealing of fission tracks in apatite 2. A quantitative analysis. Chemical Geology: Isotope Geoscience section, 65, 1-13. <https://doi.org/10.1016/0168-9622(87)90057-1>

Mihalynuk, M.G., Nelson, J., and Diakow, L.J., 1994. Cache Creek terrane entrapment: Oroclinal paradox within the Canadian Cordillera. Tectonics, 13, pp. 575-595. <https://doi.org/10.1029/93TC03492>

Monger, J.W.H., and Gibson, H.D., 2019. Mesozoic-Cenozoic deformation in the Canadian Cordillera: The record of a “Continental Bulldozer”? Tectonophysics, 757, pp. 153-169. <https://doi.org/10.1016/j.tecto.2018.12.023>

Ootes, L., Bergen, A., Milidragovic, D., Graham, B., and Simmonds, R., 2019. Preliminary geology of northern Hogem batholith, Quesnel terrane, north-central British Columbia. In: Geological Fieldwork 2018, British Columbia Ministry of Energy, Mines and Petroleum Resources, British Columbia Geological Survey Paper 2019-01, pp. 31-53.

Ootes, L., Bergen, A.L., Milidragovic, D., Jones, G.O., Camacho, A., and Friedman, R., 2020a. An update on the geology of northern Hogem batholith and its surroundings, north-central British Columbia. In: Geological Fieldwork 2019, British Columbia Ministry of Energy, Mines and Petroleum Resources, British Columbia Geological Survey Paper 2020-01, pp. 25-47.

Ootes, L., Jones, G., Schiarizza, P., Milidragovic, D., Friedman, R., Camacho, A., Luo, Y., Vezinet, A., Pearson, D.G., and Zhang, S., 2020b. Geochronologic and geochemical data from northern Hogem batholith and its surroundings, north-central British Columbia. British Columbia Ministry of Energy, Mines and Low Carbon Innovation, British Columbia Geological Survey GeoFile 2020-01, 21 p.

Ootes, L., Bergen, A.L., Milidragovic, D., and Jones, G.O., 2020c. Bedrock geology of northern Hogem batholith and its surroundings, north-central British Columbia. British Columbia Ministry of Energy, Mines and Petroleum Resources, British Columbia Geological Survey Open File 2020-02, 1:50,000 scale.

Schiarizza, P., Heffernan, S., and Zuber, J., 2001. Geology of Quesnel and Slide Mountain Terranes West of Clearwater, South-Central British Columbia (92P/9, 10, 15, 16). Geological Fieldwork 2001, British Columbia Ministry of Energy, Mines and Petroleum Resources, British Columbia Geological Survey Paper 2002-1, pp. 83-108.